Spectral reflectance of Martian meteorites:
Spectral signatures as a template for locating source region on Mars

L. A. McFADDEN[*] and T. P. CLINE

University of Maryland, Department of Astronomy, 2337 Computer and Space
Sciences Building, College Park, Maryland 20742–2421, USA
[*]Corresponding author. E-mail: mcfadden@astro.umd.edu

Abstract–We report the spectral reflectance of Martian meteorites from 0.3–2.6 microns for the purpose of cataloguing spectra and the association of their spectral properties with mineralogy and petrology. We fit the spectra to a series of overlapping, modified Gaussian absorptions using least squares fitting. The results are validated against established relationships between photon interactions with mineral chemistry and the band parameters. These resultant band parameters can be used to constrain interpretations of Martian reflectance spectra in the search for the source region of meteorites from Mars. The limitations of the fitting method are discussed.

INTRODUCTION

Martian meteorites are a group of achondritic meteorites that are distinct in terms of their mineral chemistry, oxidation-reduction state (higher oxygen fugacities), oxygen isotope composition, and radiometric ages (McSween 1985, 2002). The most direct evidence that they originate from Mars is the similarity of the isotopic composition of noble gases found as gas inclusions in impact-melted glass to the modern Martian atmospheric values (e.g., Treiman et al. 2000). The N and Ar isotope compositions fall on a mixing line between the composition of the Martian and terrestrial atmosphere (Bogard and Johnson 1983; Bogard et al. 1984).

Spectral reflectance is a remote sensing technique useful for determining the presence and abundance of certain rock-forming minerals. This method of geochemical and mineralogical analysis has the following advantages for exploration of the solar system:

1. The Sun provides an adequate light source for reflectance measurements.
2. Ground-based telescopic or spacecraft spectrometers can measure reflected light from planetary surfaces with sufficient sensitivity to determine the presence of major mafic silicates, and in some cases, a quantitative analysis of the relative abundance of common iron-bearing minerals.
3. Knowledge of mineral composition relates to the temperature at which the surface formed and provides clues to the history of the solar system, mostly in terms of differentiated versus primitive materials.
4. Laboratory spectra of mineral, rock, and meteorite samples are available to relate spectral features to the samples' mineral composition, which is independently determined.
5. Spectral reflectance is non-destructive and relatively simple.
6. Samples can be ground to simulate planetary regolith, which under certain conditions enhances the spectral contrast and promotes identification of mineral species in the spectra.

To prepare for future exploration on Mars seeking the source regions of Martian meteorites, the spectral reflectance of these meteorites is measured and reported here. The spectra are characterized by fitting modified Gaussian absorption bands to the spectra using MGM modeling (Sunshine et al. 1990). Absorption band parameters are predicted based both on their mineral chemistry and on their independently derived relationships between mineral chemistry and spectral reflectance features (e.g., Adams 1974; Cloutis and Gaffey 1991; King and Ridley 1987; Sunshine and Pieters 1990, 1993b). We interpret the fits in terms of mineral chemistry. The resulting band parameters can be used to constrain the interpretation of spectra of the Martian surface. With this approach, it is possible to test for evidence of the source region of these meteorites at the Martian surface. Locating source regions would make it possible to infer the age of that location by associating it with the age of the meteorite. The possibility of deriving an absolute age scale for the surface of Mars motivates this study.

Using spatially resolved spectra of Mars from the Phobos II mission's imaging spectrometer (ISM), Mustard and Sunshine (1995) discussed the surface composition of Mars in terms of mafic mineralogy of volcanic rocks. Examination of spectra of the Martian meteorites provides a robust example of a laboratory analysis that can be systematized to interpret reflectance spectra of planetary surfaces (e.g., Sunshine et al. 1993). The Martian meteorites have the most distinctive and readily interpretable spectral signatures of any solar system material. We discuss the possibility of using the derived band parameters to identify bedrock on Mars that might be of shergottite, nakhlite, or chassignite compositions using instrumentation on current and future missions to Mars.

METEORITE SAMPLES

Nine members of the Martian meteorite (or SNC) group are studied using spectral reflectance. Of the shergottite group, Shergotty, Zagami, Elephant Moraine (EET) 79001, Allan Hills (ALH) 84001, and Los Angeles are reported. ALH 77005, a residual magma that would be called a feldspathic hartzburgite if it were a terrestrial rock, is related to shergottites and was also measured. Nakhla and Lafayette are two nakhlites that are pyroxenite rocks. We also measure and report on Chassigny, a cumulate dunite that is the only known meteorite in this subgroup.

Shergotty fell on August 25, 1865, as a 5 kg mass in Gaya, Bihar, India. It is medium-grained diabase basalt containing pigeonite (36.3%), augite (33.5%), and maskelynite (23.3%) (e.g., Stolper and McSween 1979), though there are centimeter-scale variations. A 99 mg aliquot of powder from fragment A of the Shergotty Consortium Study (Laul 1986) is measured and used in our analyses. This sample has identical bulk chemistry to fragments B and C of the consortium study (Laul, personal communication). Stöffler et al. (1986) report pyroxene chemistry of En_{24-64} $Fs_{24-63}Wo_{12-3}$ for low-calcium pyroxene, pigeonite and $En_{40-49}Fs_{20-30}Wo_{29-34}$ for high-calcium pyroxene or augite.

Zagami fell as a 23 kg mass on October 3, 1962, in Katsina Province, Nigeria. It is a basaltic assemblage that is compositionally similar to Shergotty, composed of 36% pigeonite, 36% augite, and 22% maskelynite (Stolper and McSween 1979). The sample of Zagami used in this study is an interior sample of the meteorite, free of terrestrial weathering. It was borrowed from the collection of Candace Kohl. We measured both broken chips and crushed powder (<125 μm) derived from a few of those chips. We use the mineral chemical analyses of Zagami of $En_{51-60}Fs_{31-37}Wo_{9-12}$, pigeonite, and $En_{32-44}Fs_{21-34}Wo_{34}$, augite (Treiman and Sutton 1992). We assume its composition is homogeneous from sample to sample, an assumption deemed reasonable (McSween, personal communication) and supported by previously published petrological studies (e.g., Smith et al. 1983; Treiman and Sutton 1992).

EET 79001 was found in December 1979 near Reckling Peak, Antarctica, as a 7.94 kg object. It contains two primary lithologies in planar contact that are likely to represent sequential lava flows from successive pulses of magma. Lithology A is composed primarily of pigeonite (En_{61-45} $Fs_{29-44}Wo_{10-11}$), augite ($En_{51-41}Fs_{24-28}Wo_{25-30}$), and maskelynite as a groundmass with porphyritic texture. Lithology B contains more augite than lithology A and is non-porphyritic in texture. Lithology C is a dark, shock-melted glass from within lithology A (McSween and Jarosewich 1983). Our samples are on loan from the National Institute of Polar Research, Japan. We measured two polished thin sections of EET 79001,79 containing both lithologies A and B, and a third subsample, EET 79001,73 including lithology A and shock-melted glass of the same composition, known as lithology C. The polished thin sections were placed on top of the halon reference sample to obtain a reflectance spectrum. Powdered samples (<150 μm) of lithology A and B that were taken from near EET 79001,79 were also measured. These are the same samples used for mineralogical and petrological studies carried out by McSween and Jarosewich (1983). Spectra of powders of lithology A and B are analyzed in Sunshine et al. (1993). We employ the MGM model, fitting the approach to the spectra of this meteorite as a check to our procedures and analysis, and expand our analysis to include spectra from discrete areas on thin sections.

ALH 84001 consists of 97% orthopyroxene with minor phases including chromite, maskelynite, augite, apatite, pyrite, and carbonates in a cumulate texture. Orthopyroxene composition is uniform at $En_{69.4}Fs_{27.3}Wo_{3.3}$ (Mittlefehldt 1994). Its association with Martian meteorites is derived from its oxygen isotope composition (Clayton 1993) and petrographic analysis (Mittlefehldt 1994). It was studied by McKay et al. (1996), who reported possible evidence of fossil life. ALH 84001, splits 92 and 271, were loaned to Janice Bishop by the Meteorite Working Group and measured at RELAB. Spectral reflectance measurements of chips and powder from these samples were measured and analyzed in terms of major mineral composition, as well as for the presence of minor constituents in reflectance spectra (Bishop et al. 1998a, 1998b). We use these previously published spectra for our analysis of absorption band parameters of this meteorite.

ALH 77005 was found in 1977 in Allan Hills, Antarctica, as a 482 g mass. The meteorite consists of poikilitic pyroxenes which are mostly low-calcium orthopyroxene, but contain both pigeonite and augite, enclosing olivine and chromite with interstitial olivine, maskelynite and minor pyroxenes, chromite, ilmenite, sulfides, and phosphates (McSween, Taylor, and Stolper 1979). The mean olivine composition is Fo_{74} and the low-calcium pyroxene ranges in composition between $En_{82}Fs_{16}Wo_2$ and $En_{58}Fs_{30}Wo_{12}$ (McSween et al. 1979; McSween 1985). Sample ALH 77005,112 is a broken chip slightly larger than 1 cm loaned to this author by Johnson

Table 1. List of samples measured and analyzed with MGM fitting.

Sample	Description	RELAB ID	RELAB File
Shergotty	powder <125 μm	LM-LAM-021	C1LM21
Zagami	powder <125 μm	MB-LAM-049-P	CPMB49
EET 79001,79 lith. A	powder <150 μm	LM-LAM-007-PA	C1LM07
EET 79001,79 lith. A	thin section	LM-LAM-007-79	T5LM07
EET 79001,79 lith. B	powder <150 μm	LM-LAM-007-PB	C2LM07
EET 79001,79 lith. B	thin section	LM-LAM-007-79	T7LM07
EET 79001,73 lith. A	thin section	LM-LAM-007-73	TALM07
EET 79001,73 lith. C	thin section	LM-LAM-007-73	TCLM07
ALH 84001,92	powder <125 μm	MT-TXH-002-3	C3MT02
ALH 77005	powder	Submitted to PDS	
ALH 77005,112	chip	LM-LAM-009-B	CBLM09
ALH 77005,112	chip	LM-LAM-009-C	CCLM09
ALH 77005,112	chip	LM-LAM-009-D	CDLM09
Los Angeles	<1000 μm	MT-JFM-005	C1MT05
Chassigny	powder <300 μm	MR-MJG-104	MGP075
Nakhla	powder ~300 μm	MR-MJG-102	MGP071
Lafayette	powder <100 μm	LM-LAM-023	C1LM23

Space Center for this study. We measured different areas of the chip, including fusion crust. A powdered sample ground to <150 μm was also measured.

Los Angeles is a basaltic shergottite found in October 1999, comprising two stones with a combined mass of 698 g. It consists of almost 50% maskelynite and 40% pyroxene, with approximately 10% minor constituents. Most of the rock is subophitic in texture (Rubin et al. 2000). Pyroxene compositions range from $En_{50-6}Fs_{81-33}Wo_{12-41}$ (Xirouchakis et al. 2002). A small sample of course-grained powder (<1000 μm) of the Los Angeles meteorite was measured by Mustard at RELAB and used here in our analysis of absorption band parameters.

Chassigny fell on October 3, 1815, in Haute Marne, France. The four kilograms recovered are a cumulate rock primarily consisting of olivine (Fo_{68}) with some augite and orthopyroxene (e.g., Floran et al. 1978). Our sample was ground to ~300 μm and first reported by Gaffey (1976) from a sample on loan from the Field Museum, Chicago, Illinois.

Nakhla fell June 28, 1911, in Abu Hommos, Alexandria, Egypt. Forty stones were recovered. This meteorite is a cumulate rock consisting primarily of augite and about 15% olivine (Bunch and Reid 1975; Mikouchi and Miyamoto 1998). Spectra were first measured from a sample borrowed from the Harvard collection of meteorites and first reported by Gaffey (1976). We performed band fits on Gaffey's sample described as coarsely ground (~300 μm) that were remeasured at RELAB (Table 1). Smith et al. (1983) report mineral chemistry for Nakhla augite of $En_{28-40}Fs_{22-34}Wo_{37-39}$. Bunch and Reid (1975) report olivine compositions of $Fo_{32}Fa_{68}$.

Lafayette was found in Tippecanoe County, Indiana, before 1931. The meteorite is a clinopyroxenite containing augite, ferropigeonite, and olivine (e.g., Smith et al. 1983) that has undergone late magmatic and subsolidus diffusion controlled by location in a cooling pile of cumulate rock (Harvey and McSween 1992). As a find, it contains considerable terrestrial weathering. The sample measured was loaned from the collection of Nishizumi as powder (<100 μm), which is the Field Museum's sample Me 2116 (Nishizumi, personal communication). Chemical analysis of this sample is by Lodders (1998). Electron microprobe analysis of olivine yields $Fo_{33}Fa_{67}$ and augite $En_{37-38}Fs_{22-23}Wo_{38-41}$ (Smith et al. 1983) as primary mineral components.

MEASUREMENT AND ANALYSIS METHODS

The spectra reported here were measured with the RELAB reflectance spectrometer (Pieters 1983), except for the powdered sample of ALH 77005 that was measured using the laboratory spectrogoniometer at Planetary Geosciences Division, University of Hawaii (e.g., Singer 1981). Visible and near-IR spectra of ALH 77005 were acquired with a cooled CVF spectrometer with measurements made at wavelength intervals of 6–21 nm. Standard setup for both the University of Hawaii and RELAB measurements includes an incidence angle of 30° and a nadir, 0° angle of emission. RELAB spectra were measured at 5 nm intervals from 0.300–2.600 μm relative to Halon, a material of plastic spheres manufactured to be close to a perfect reflector (Weidner and Hsia 1981). A correction based on the NBS calibration of Halon is applied to all spectra measured at RELAB. A quartz halogen lamp is the light source used with a Jarrel Ash half-meter monochrometer. Three spectra, Shergotty, Nakhla, and Lafayette, were measured to 3.5 μm. Spectra are available in the RELAB database at http://www.planetary.brown.edu/relab and are also listed in Table 1. The spectrum of ALH 77005 powder will be submitted to the Planetary Data System's Small Bodies Node at http://pdssbn.astro.umd.edu.
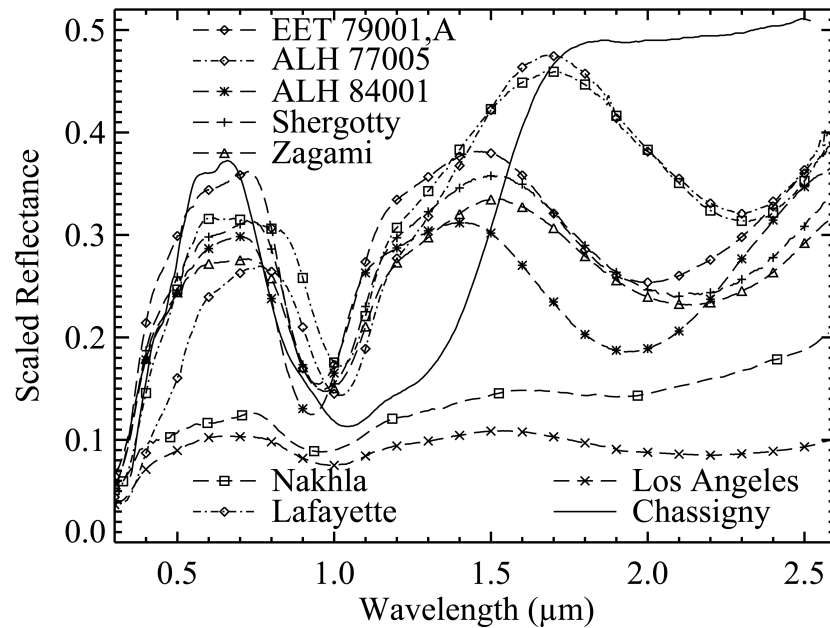
Fig. 1. Reflectance versus wavelength of powdered samples of Martian meteorites included in this study using RELAB spectrometer, i = 30°, e = 0°. ALH 77005 was measured at Planetary Geosciences spectrometer, University of Hawaii, with the same geometry. Scaled reflectance is relative to halon.
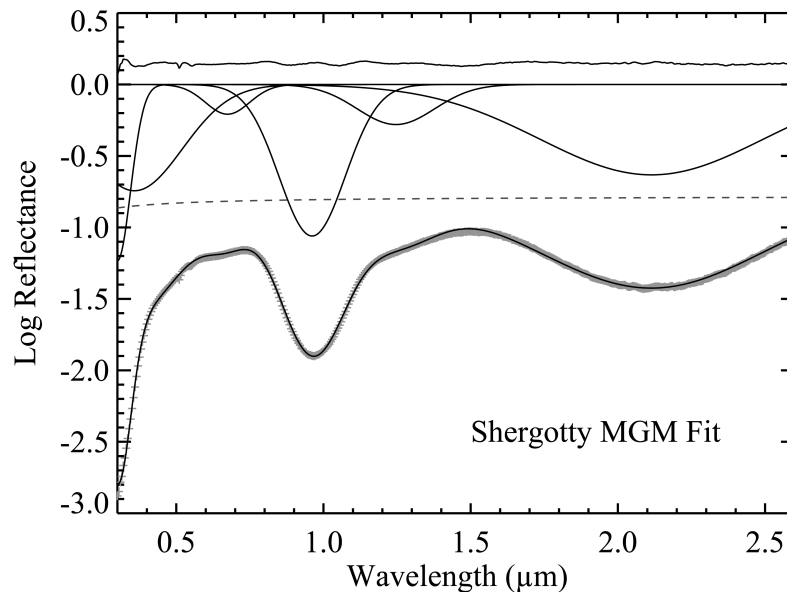

Fig. 2a. MGM band fit of Shergotty, a basaltic shergottite meteorite powder represented by one pyroxene. Top plot is the residuals from the fit. The second set of plots is the fitted bands. The dotted line is the continuum removed before fitting. The bottom plot is the measured spectrum (overlapping "+"s) with the fitted spectrum as a solid line. The non-constant residuals versus wavelength with peaks that are offset from the strongest band around 1 μm indicate that additional bands should be included in the fit.

BAND ANALYSIS METHOD

The fitting routine used for characterizing absorption band parameters in this study was developed by Sunshine et al. (1990). The approach has been used successfully for multiple purposes. Sunshine et al. (1990) developed the

modified Gaussian method (MGM) and demonstrated that unconstrained modified Gaussian band analyses correctly identify the band center and strength of superimposed absorption bands for pyroxenes and olivines and mixtures of orthopyroxene and clinopyroxene. In Sunshine and Pieters (1993a), all three band parameters—position, width, and
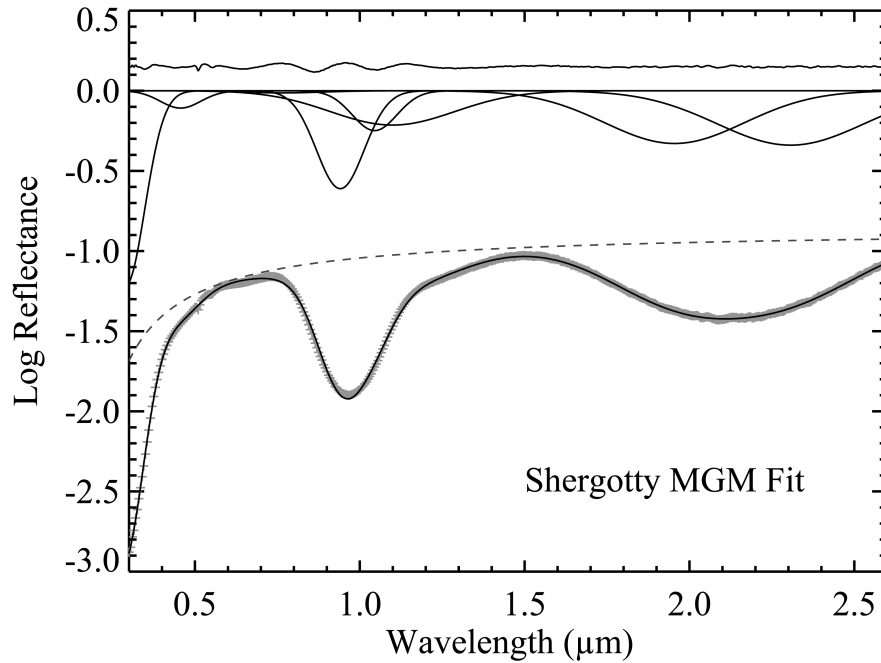
Fig. 2b. MGM band fit of Shergotty powder represented by two pyroxenes. The fit has non-constant residuals indicative of a poor fit, and the width of the band at 1.10 μm is not physically realistic. The fit does not pass validation criteria.
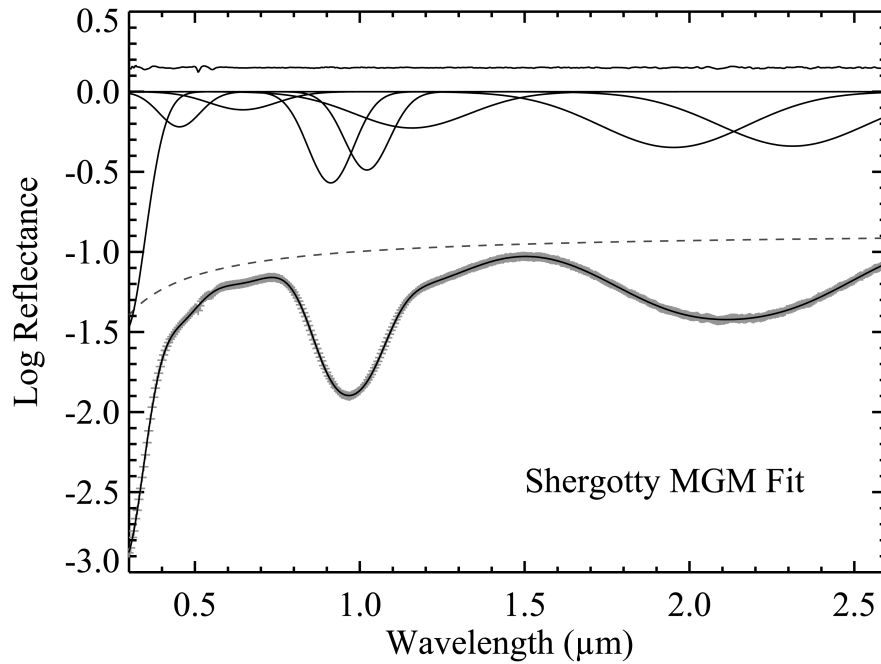

Fig 2c. Final MGM band fit of powdered Shergotty with smooth residuals including two pairs of pyroxene bands. The relative band depths of the two pairs of pyroxene bands and the M1 band at 1.14 micron accurately represent the meteorite.

relative band strength derived from MGM fits—are shown to be independent of particle size, and can be used to estimate composition of the components and their modal abundance. Samples with different textures, zoning, and exsolution were also investigated and characterized. A comparison of the geochemical analysis of the shergottite EET A79001 with remote sensing spectral analysis and MGM band fitting was carried out by Sunshine et al. (1993) without constraining band parameters. MGM analyses of forsterite-fayalite solid solution series were analyzed (Sunshine and Pieters 1998) and shown to provide systematic relationships related to composition. In the case of olivine spectra, constraints

derived from mineral physics is required to produce physically meaningful band parameters.

Each spectrum presented here is first described qualitatively from visual inspection (Fig. 1). Each sample's spectrum is then fit to a linear combination of modified Gaussian absorption bands superimposed on a continuum (e.g., Fig. 2a). In this study, we constrained the fits based on mineral physics because our objective is to arrive at a set of band parameters that can be used to interpret spectra of the Martian surface. Each absorption band is characterized by three parameters: band center, measured in nanometers, width, measured in nanometers as full width at half maximum height (FWHM), and depth, measured relative to a continuum-removed spectrum in units of natural log of reflectance. The starting parameters used to initiate the linear least squares fit are derived from knowledge of the mineral composition of the sample and knowledge of the relationships between absorption band parameters and mineral chemistry. The continuum is defined as a straight line in energy space, an empirical approach necessitated both by the absence of a realistic physical model for the continuum and because the mineralogical information is contained in the absorption bands and not the background continuum. The absorption bands are modeled in log reflectance and energy space. The model spectrum is compared with the measured spectrum by the least squares method until the total RMS error is below 0.009 and a net change in residual error between two steps is less than 1×10^{-5}.

In examining the results of a fit, the likelihood of the presence of additional absorption bands is assessed based on the character of the residual spectrum and mineralogy and petrology of the meteorite following the procedure of Sunshine et al. (1993). In some cases, absorption bands are added corresponding to additional mineral components, and the model is run again. The fitting ends when the resulting band parameters can be associated with the chemical composition of the solid solution series for pyroxene (e.g., Adams 1974, 1975; Hazen et al. 1978; Cloutis and Gaffey 1991; Sunshine et al. 1990), and olivine (King and Ridley 1987; Sunshine and Pieters 1990, 1993b). These results are shown in Figs. 3a–c for meteorites in which pyroxene dominates the spectrum. The resulting band parameters are considered validated against the physics of light interactions with the mineral of a specific composition when the band parameters fall within the laboratory calibrations of constituent minerals and the residuals are small and constant.

It is necessary to place constraints on the continuum. For example, the continuum slope is always positive for the spectrum of a powdered sample. It was also found that when the continuum is tangent to the spectrum, the band parameters do not conform to known relationships between band parameters and mineral composition. We discuss this in the fitting of Shergotty below.

The focus here is on the bands at 1.0 and 2.0 μm that shift

with iron and calcium chemistry. The resulting band parameters are good indicators of the petrology of the sample under study. Spectra in which olivine dominates have a composite band consisting of three components in the 1 μm region with no 2 μm band. Chassigny (Fig. 1) is an example. We describe each meteorite spectrum and list its band parameters. When high spectral and spatial resolution reflectance spectra of the Martian surface become available, the band parameters derived here can be used as a test for similar mineralogical composition. If the source regions of these meteorites can be located on Mars, an absolute age scale for the planet can be derived.

RESULTS AND VALIDATION

Spectral Parameters and Their Physical Significance

All the spectra have a strong absorption edge into the ultraviolet end of the spectrum referred to as a metal-oxygen charge transfer band (Fig. 1). And with the exception of Chassigny, all the spectra show prominent absorption bands at 1 and 2 μm. Chassigny, predominantly olivine, does not have any 2 μm bands. Weak features are superimposed on the UV absorption edge of most of the samples. The position, width, and strength of the most prominent absorption bands correspond to electronic transitions of iron in d-orbital electrons in silicate crystal structures. The values derived from MGM analysis of powdered samples are listed in Tables 2–10 for each sample. In the Martian meteorites, mafic minerals, pyroxene, and olivine, dominate both the spectrum and the meteorite itself. In general, the grain size of a sample and its texture can either enhance or suppress the spectral signatures in reflected light. As most of the Martian meteorites have large grains (in the millimeter range) and contain only a few opaque minerals, high reflectance values and strong absorption bands are produced in reflectance spectra. These factors support the use of spectral reflectance to search for the source region of these meteorites on Mars.

The UV band edge is an intervalence charge transfer (IVCT) absorption extending into the ultraviolet (e.g., Burns 1993). Electrons move between the central transition metal cations, Fe, and the O ions at the corners of silica tetrahedra. Whereas these bands are a factor of 10–1000 times stronger than other absorptions, they are ubiquitous in mafic silicate spectra. The energy of the transitions does not fall completely within the spectral range of the spectrometer, making it impossible to characterize the band minimum or width. For these reasons, no systematic relationships between mineral structure and band parameters have been derived for the UV absorption edge. Generally speaking, a strong charge transfer absorption indicates a moderate to high abundance of iron and a low abundance of any opaque material absorbing in the UV. A weak charge transfer absorption is indicative of either a low abundance of iron in the material or the presence of an opaque

Table 2. Shergotty powder band parameters.

Band	Mineral	Site	Center (nm)	FWHM	Strength
1	pyx	CT	294.57	137.76	−1.50
2	pyx	CF	453.15	130.07	−0.20
3	pyx	CF	679.76	264.01	−0.11
4	pig	M2	910.13	162.21	−0.67
5	aug	M2	1020.12	159.45	−0.56
6	aug	M1	1144.76	355.06	−0.25
7	pig	M2	1937.69	461.80	−0.42
8	aug	M2	2295.60	480.66	−0.42

pyx = pyroxene; pig = pigeonite; aug = augite; FWHM = full width half maximum.
RMS error = 0.00564.

Table 3. Zagami powder band parameters.

Band	Mineral	Site	Center (nm)	FWHM	Strength
1	pyx	CT	290.20	135.90	−1.32
2	pyx	CF	444.31	145.02	−0.16
3	pyx	CF	703.96	376.47	−0.14
4	pig	M2	921.69	162.08	−0.50
5	aug	M2	1030.86	161.17	−0.43
6	aug	M1	1166.62	400.30	−0.23
7	pig	M2	1970.28	548.59	−0.33
8	aug	M2	2324.74	542.63	−0.31

pyx = pyroxene; pig = pigeonite; aug = augite; FWHM = full width half maximum.
RMS error = 0.00252.

component that absorbs at wavelengths below 0.4 μm. The UV absorption band can become stronger by the presence of iron oxide, a product of terrestrial weathering meteorite samples. The Martian meteorites do not weather as readily or as rapidly as meteorites containing metallic iron; therefore terrestrial weathering and its spectral effects are not a concern for this study. The strong UV absorption bands are consistent with significant amounts of iron in the mafic silicates and low abundance of opaque minerals, such as chromite, ilmenite, or iron oxides in the Fe^{3+} state that are present as trace elements in Martian meteorites.

The weak and narrow absorption features superimposed on the UV charge transfer edge have been attributed to transition elements in both pyroxene and olivine. They are designated as crystal field (CF) transitions in Tables 2–10. They are weak bands that are spin-forbidden. The analysis of these bands can be important for determining the redox state of the starting composition (e.g., Hale et al. 1999). An effort to associate specific cations with bands in the visible was not successful. Cloutis (2002) arrived at the same conclusion for terrestrial pyroxenes.

The 1 and 2 μm bands are composites of overlapping bands that violate the rules of symmetry forbidding transitions between cations of the same sign. They are LaPorte forbidden electronic transitions of iron cations in asymmetric M1 and M2 octahedral crystal sites (e.g., Burns 1993; Adams 1974; Rossman 1980). Weaker bands both longward and shortward of the strong M2 band in the 0.9– 1.0 μm region are M1 bands that appear in all pyroxenes (e.g., Burns 1993; Sunshine and Pieters 1993a). We observe in the

spectra presented here that the M1 bands are always weaker than the M2 bands, as has been observed previously (e.g., Rossman 1980; Sunshine et al. 1993). The M1 bands are stronger in high-Fe and Ca pyroxenes than in low-Fe and low-Ca orthopyroxenes, as will be demonstrated in the Martian meteorites below.

Shergotty

Three absorption bands dominate the spectrum of powdered Shergotty, a UV absorption edge and a 1 and 2 μm band (Fig. 1). A mid-visible plateau lies between 0.6 and 0.85 μm and a change in slope on the long wavelength edge of the 1 μm band between 1.2 and 1.5 μm modulates the near-IR maximum, which peaks at 1.490 μm. We present three different fits of Shergotty to demonstrate the process of arriving at a physically meaningful fit of the spectrum.

Our first start-up file was developed by eye and resulted in six overlapping Gaussian bands (Fig. 2a). The strongest bands at 0.96 and 2.11 μm result from Fe^{2+} electronic transitions in distorted M2 sites. The band at 1.25 μm is due to Fe^{2+} in the M1 site in low-calcium pyroxene (e.g., Rossman 1980). Evidence that additional bands should be included is found by examining the residuals in Fig. 2a. These show periodic variations, suggesting a better fit could be found by adding more absorption bands for the spectrum of EET 79001, as discussed in Sunshine et al. (1993). The literature on the mineralogy of Shergotty (Stolper and McSween 1979; Laul 1986) indicates that there are two pyroxenes, so the fit with one pair of pyroxene bands is not representative of the
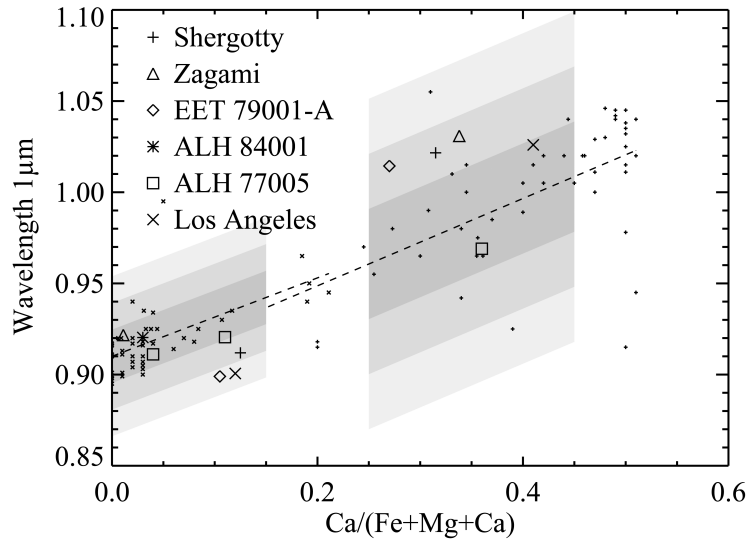
Fig. 3a. Wavelength position of 1 μm pyroxene band versus Ca/(Ca + Fe + Mg). Two separate, straight dashed lines represent the least squares fit of band centers of terrestrial pyroxenes (small "x"s) versus Ca/(Ca + Fe + Mg) in low-Ca and high-Ca pyroxenes from Cloutis and Gaffey (1991). Shaded regions represent ranges 1 σ, 2 σ, and 3 σ intervals from the mean. These intervals are considered the expected region for band centers derived from MGM fits of Martian meteorites using mineral chemistry derived from independent geochemical analysis. The resultant band centers from MGM fits of spectra of powdered samples analyzed in this paper are plotted in large symbols noted in the figure legend. Band centers are within 2 σ of the mean of terrestrial band centers.
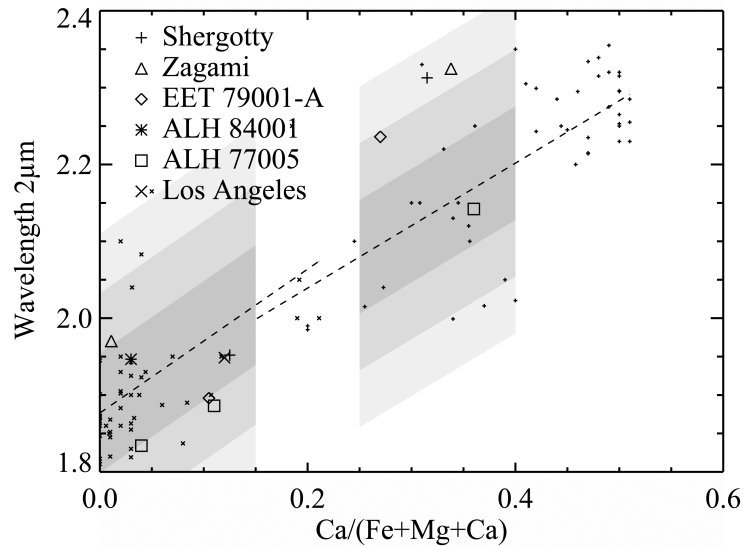

Fig. 3b. Wavelength position of 2 μm pyroxene band versus Ca/(Ca + Fe + Mg). The two straight lines (dashed) represent the least squares fit of band centers (small "x"s) of low-Ca and high-Ca terrestrial pyroxenes versus Ca/(Ca + Fe + Mg) (Cloutis and Gaffey 1991). Shaded regions represent ranges 1 σ, 2 σ, and 3 σ intervals from the mean. They are considered the expected region for band centers that are associated with pyroxenes found in Martian meteorites. Data on the x-axis are from geochemical analyses noted in the text. All powdered samples fall within 3 σ of the mean of terrestrial band centers.

sample's mineralogy. There is both a mathematical and a physical reason for rejecting this fit of Shergotty.

The next step was to add an additional pair of bands around 1 and 2 μm and to move the starting band centers to values derived from Figs. 3a and 3b, based on the average pyroxene chemistry in Shergotty, of $En_{24-64}Fs_{24-63}Wo_{12-13}$ and $En_{40-49}Fs_{20-30}Wo_{29-34}$, determined by Stöffler et al.

(1986) and previously determined band centers from terrestrial pyroxenes. The residuals of this MGM fit have wavelength-dependent and varying residuals (Fig. 2b), and the width of the band at ~1.2 μm is too broad to be physically meaningful. We reject this fit on both mathematical and physical grounds as well.

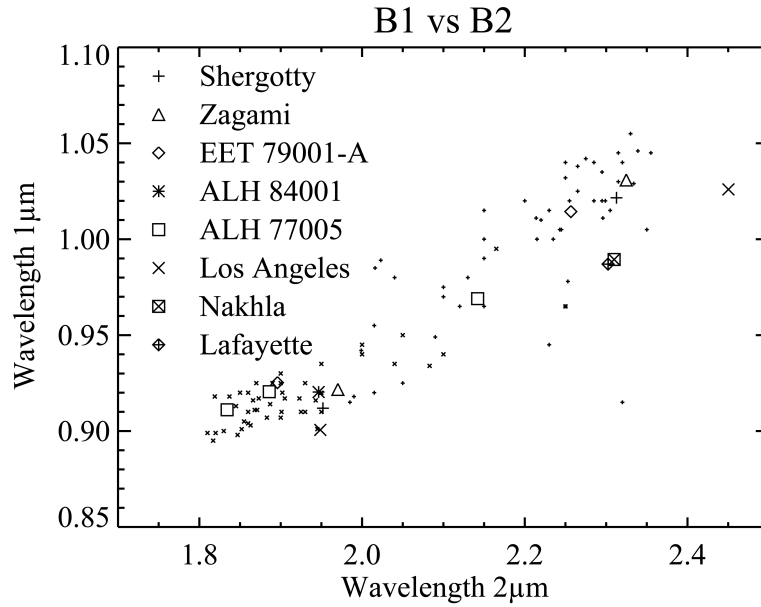The final step was to raise the continuum so it was not

B1 vs B2

Fig. 3c. Pyroxene 1 μm versus 2 μm plot (also called B1 versus B2) with terrestrial pyroxenes as small "x"s and Martian meteorites in larger symbols as noted in legend. Band pairs falling within the background range are realistic band centers for pyroxene compositions. This plot provides another check on the validity of band centers.
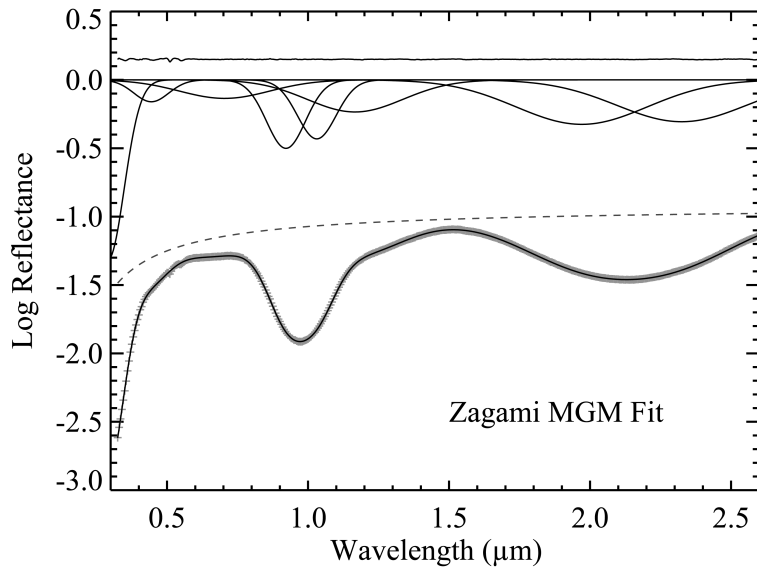

Fig. 4. MGM band fit of Zagami powder containing pigeonite, augite, and maskelynite. Plots are as described in Fig. 2.

tangent to the spectrum at any point. We allowed the mathematics to arrive at a fit (Table 2, Fig. 2c) representative of the pyroxene mineralogy of Shergotty ($En_{24-64}Fs_{24-63}$ Wo_{12-13} and $En_{40-49}Fs_{20-30}Wo_{29-34}$ (Stöffler et al. 1986). The band centers plot within the pyroxene range as shown in Fig. 3c. The regions, shown in three gradations of gray in Figs. 3a and 3b, represent 1 σ, 2 σ, and 3 σ ranges from the linear function describing the band center as a function of elemental ratio in pyroxene mineral chemistry derived from laboratory measurements of terrestrial pyroxenes. The

position of the 1 μm bands fall within 2 σ of the relationship between chemistry and band centers (Fig. 3a). In Fig. 3b, the band positions for Shergotty pyroxenes are within 1 σ and 3 σ of the mean for the low-calcium and high-calcium 2 μm bands, respectively. We conclude that the fit in Fig. 2c is representative of the structure of the pyroxenes in Shergotty.

The strong UV absorption edge at 0.295 μm is a metal-oxygen charge transfer band and indicates a high abundance of mafic silicates without optically significant opaque minerals. The band at 0.453 μm could be due to iron or

Table 4. EET 79001 powder and thin sections band parameters.

Sample	Band	Mineral	Site	Center (nm)	FWHM	Strength	ΔCenter[a]	ΔFWHM	ΔStrength
Powder of lith. A.	1	pig	M1	899.58	161.67	−0.6	n.d.	n.d.	n.d.
	2	aug	M2	1000.41	162.3	−0.48	n.d.	n.d.	n.d.
	3	aug	M1	1129.47	412.09	−0.22	n.d.	n.d.	n.d.
	4	pig	M2	1895.31	499.05	−0.37	n.d.	n.d.	n.d.
	5	aug	M2	2236.96	542.81	−0.3	n.d.	n.d.	n.d.
Lith. A. T. S.	1	pig	M1	909.38	160.26	−0.46	0.011	−0.009	−0.264
	2	aug	M2	998.72	163.62	−0.29	−0.002	0.008	−0.494
	3	aug	M1	1163.24	433.45	−0.14	0.029	0.051	−0.444
	4	pig	M2	1843.86	495.14	−0.1	−0.028	−0.008	−1.149
	5	aug	M2	2101.33	498.92	−0.13	−0.063	−0.084	−0.791
Lith. B. T. S.	1	pig	M1	911.03	160.13	−0.42	0.013	−0.010	−0.353
	2	aug	M2	998.93	162.6	−0.26	−0.001	0.002	−0.595
	3	aug	M1	1170.59	429.23	−0.15	0.036	0.041	−0.378
	4	pig	M2	1784.51	500.33	−0.11	−0.060	0.003	−1.083
	5	aug	M2	2092.44	494.21	−0.15	−0.067	−0.094	−0.667
Dark inclusion	1	pig	M1	916.08	169.57	−0.38	0.018	0.048	−0.449
	2	aug	M2	1022.93	170.85	−0.23	0.022	0.051	−0.704
	3	aug	M1	1195.1	507.34	−0.32	0.056	0.207	0.370
	4	pig	M2	1785.7	551.95	−0.18	−0.060	0.101	−0.691
	5	aug	M2	2168.36	630.46	−0.15	−0.031	0.149	−0.667

[a] $\Delta\text{center} = 2 * \dfrac{\text{powder} - \text{T. S.}}{\text{B\#powder} + \text{B\#T. S.}}$, same for ΔFWHM and Δstrength

chromium in pyroxene (Cloutis et al. 2004; Burns 1993). There are usually additional bands at 0.63 and 0.66 μm in chromium-rich pyroxenes that are not found in Shergotty's spectrum. Hence, we cannot associate the 0.453 μm band with chromium. There is a band at 0.680 μm, but only a single band, and its associated ion is not clear. The 0.910 μm and the 1.938 μm bands are assigned to low-Ca pyroxene (pigeonite) in the M2 site, while the 1.020 μm and 2.296 μm bands are transitions in higher Ca augite. The band at 1.144 μm is created by a M1 site in augite. A band at this position is often attributed to iron in plagioclase, but that is not the case in this sample because Shergotty plagioclase has been shocked to maskelynite, which has a very weak band around 1.3 μm that would be swamped by any pyroxene signature (Pieters 1996). Absorption bands in oriented single crystals of pyroxene (Burns 1993) show M1 sites in the 1.1–1.2 μm region. In this spectrum, all absorption bands can be attributed to pyroxenes. None of the bands are attributed to maskelynite, the shocked polymorph of plagioclase, which does not have a high enough absorption coefficient to be spectrally detected, despite the fact that the meteorite is 9.8% by weight and 12.5% by volume plagioclase (Lodders 1998).

Zagami

The spectrum of a powder (<125 μm) of Zagami was measured. Three absorption bands are prominent: the UV absorption band and the 1 and 2 μm bands (Fig. 4). Two very weak and narrow bands are superimposed on the UV band at 0.505 and 0.56 μm; these bands were not included in the MGM fitting; however, they can be seen in the residuals. A broader yet still weak band at approximately 0.704 μm shifts the maximum visible reflectance to 0.28 at approximately 0.725 μm.

We used the fitted parameters of Shergotty as a startup file for Zagami because its mineralogy is similar to Shergotty. The best fit has eight absorption bands as well as RMS residuals of 0.003 (Fig. 4, Table 3.). The 1 μm bands fall within 1 and 2 σ of the relationship between band center and elemental ratio (Fig. 3a). They also fall within 2 to 3 σ for the 2 μm band versus elemental ratio (Fig. 3b). The centers for band 1 and band 2 are plotted in Fig. 3c, where they fall within the pyroxene region of the band-band plot. We consider this fit to be validated against Zagami's mineralogy.

Table 5. ALH 84001 powder band parameters.

Band	Mineral	Site	Center (nm)	FWHM	Strength
1	pyx	CT	290.78	115.33	−1.04
2	pyx	CF	362.96	328.20	−0.56
3	pyx	CF	671.60	173.30	−0.13
4	opx	M2	920.34	203.41	−1.02
5	opx	M1	1166.58	356.13	−0.25
6	opx	M2	1946.59	665.47	−0.72

pyx = pyroxene; opx = orthopyroxene; FWHM = full width half max.
RMS error = 0.00437.

EET 79001

Powdered samples of this shergottite were the subject of a spectral reflectance study by Sunshine et al. (1993) comparing spectroscopic analyses with petrological and geochemical studies. In that study, it was clearly shown that reflectance spectra of lithologies A and B are resolved into different modified Gaussian bands associated with the specific mineral chemistry of each lithology. Band positions (Table 4) of powder of lithology A fall within 3 σ of the band center versus Ca/(Fe + Mg + Ca) relationships (Figs. 3a and 3b) and on the pyroxene trend of the band-band plot (Fig. 3c). These validated parameters are listed in Table 4.

We measured spectra of regions of thin sections EET 79001,79 and EET 79001,73 (Fig. 5) and determined MGM band fits of the different regions marked in the figure. The fitted band parameters change with location on the thin section as demonstrated by the reflectance spectra (Figs. 6a and 6b, Table 4). The differences between band fits of powdered lithology A and a region of the thin section of the same lithology is calculated as the difference between the parameter determined for the powder minus that of a specific location on the thin section and divided by the average of the two (Table 4). The values measured as a percent of the powder's parameters are between 0%–6% for band center and 0%–8% for band width. The band strength, however, is stronger in the powdered spectrum by at least 25% and as much as 115% (Table 4).

All band positions range between 0–6% from the mean parameters derived from all fits. The small variation between band fits of powdered samples and thin sections for band centers and widths demonstrates that spectral reflectance of thin sections placed on top of the reference standard, halon, can be used to determine band parameters that are accurate to better than 10%. The parameters can then be interpreted in terms of the minerals present within the aperture to within 10%. Measuring spectral reflectance of specific regions of a thin section can be used to disentangle mineralogical heterogeneity within a sample.

Lithology C is the glassy mesostasis from EET 79001,73 (Fig. 5). The spectrum increases in reflectance with increasing wavelength (Fig. 6b). A 1 μm band is present with no apparent 2 μm band and no superimposed weak features on
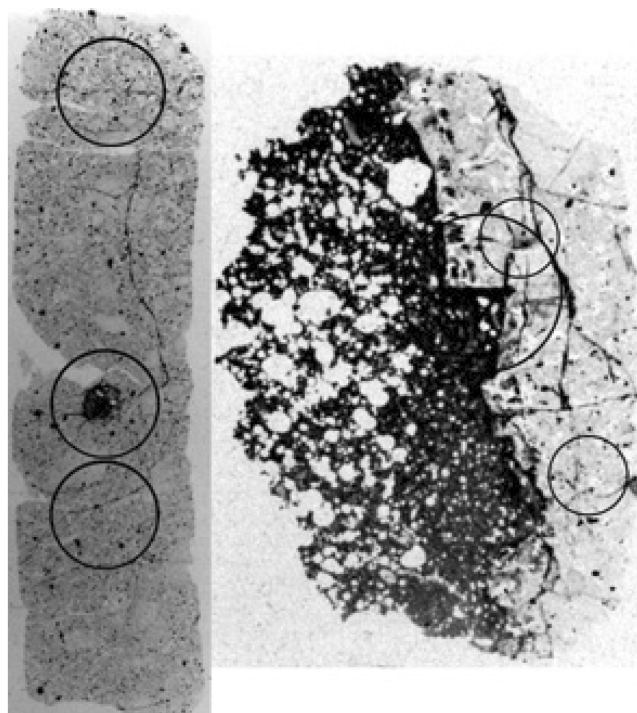

Fig. 5. Thin section of EET 79001,79 (left). Top circle is lithology A, middle is lithology B with inclusion, bottom is lithology B. EET 79001,73 (right). Small circle on bottom right is lithology A, large circle in the middle overlapping bright and dark boundary is lithology A + C, dark region with no marking is lithology C. Spectra of these areas are in Figs. 6a and 6b.

the continuum. This spectrum is modeled with seven weak bands after removal of the continuum (Fig. 7). That the bands can be modeled with low residuals suggests that remnant crystal structure of pyroxene octahedra is present in this glassy material. That the bands are at least 37% and as much as 70% weaker as well as at least 5% and as much as 20% broader than powder indicates significant disorder in the material, consistent with its glassy state.

ALH 84001

We report band positions from MGM fitting (Fig. 8). We started spectrum fitting with a low-calcium pyroxene start-up file consistent with its dominant mineralogy of orthopyroxene. The residuals in the 1 μm region were not constant as they were in the 2 μm region. Two bands were added for a high-calcium pyroxene that is usually found in shergottite meteorites. The resultant fits fell in the low-calcium pyroxene range of the band-band plot. Residuals in the 1 μm region were still not constant. Additional fits produced bands that were not realistic in terms of band width (excessively wide) and/or depth relationships (overly strong or too weak bands). None of the fits containing two pyroxene bands were realistic in terms of band parameters and chemical mineralogy relations. We conclude that this

Table 6. ALH 77005 powder band parameters.

Band	Mineral	Site	Center (nm)	FWHM	Strength
1	pyx	CT	225.94	177.68	−0.70
2	pyx	CF	471.00	123.34	−0.15
3	pyx	CF	630.41	190.60	−0.22
4	ol	M1	849.10	217.68	−0.21
5	pyx	M1	911.08	204.79	−0.13
6	pyx	M2	920.52	204.90	−0.10
7	pyx	M2	969.01	205.06	−0.13
8	ol	M2	1048.89	183.51	−0.21
9	ol	M1	1231.91	460.37	−0.36
10	pyx	M2	1834.12	699.21	−0.14
11	pyx	M2	1885.91	702.06	−0.12
12	pyx	M2	2142.07	707.01	−0.11

pyx = pyroxene; ol = olivine; FWHM = full width half max.
RMS error = 0.00951.

Table 7. Los Angeles powder band parameters.

Band	Mineral	Site	Center (nm)	FWHM	Strength
1	pyx	CT	315.80	101.87	−0.46
2	pyx	CF	452.64	174.14	−0.08
3	pyx	CF	704.65	146.16	−0.06
4	pyx	M2	900.59	200.25	−0.24
5	pyx	M2	1025.97	191.85	−0.24
6	pyx	M1	1213.09	450.59	−0.27
7	pyx	M2	1948.65	705.23	−0.36
8	pyx	M2	2450.33	672.97	−0.35

pyx = pyroxene; FWHM = full width half max.
RMS error = 0.00363.

Table 8. Chassigny powder band parameters.

Band	Mineral	Site	Center (nm)	FWHM	Strength
1	ol	CT	291.00	144.21	−2.60
2	ol	CF	454.69	132.06	−0.51
3	ol	CF	607.56	102.77	−0.13
4	ol	M1	865.29	233.09	−0.71
5	ol	M2	1035.97	200.48	−0.65
6	ol	M1	1244.30	446.61	−1.11

ol = olivine; FWHM = full width half max.
RMS error = 0.00852.

sample contains very little high-calcium pyroxene, augite. Six bands are fit (Table 5); the bands at 0.92 and 1.94 μm are due to low-calcium orthopyroxene in M2 octahedral sites. The results of this fitting are consistent with Mittlefehldt's petrological study of the meteorite. It was misidentified as a diogenite upon initial classification and was identified as Martian from its petrological relationships and oxygen isotope ratios (Clayton 1993). Augite exists as an accessory mineral, and if it is present in the sample here, it is in amounts too small to be detected, probably <5% by mass. The predominant pyroxene is a low-calcium orthopyroxene. Band parameters (Table 5) are consistent with the mineralogy reported by Mittlefehldt (1994). They are

physically validated by being within 1 σ of the pyroxene trends (Figs. 3a and 3b) and falling on the orthopyroxene end of the band-band plot (Fig. 3c).

ALH 77005

Spectra of ALH 77005 (Fig. 9) were taken on four parts of the chip sample designated its external face, internal blackish face, internal fresh face, black part of internal face, and powder (<100 μm). The internal fresh face has the strongest absorption bands in the UV, 1 and 2 μm regions. Peak reflectance is at 0.72 μm and the 2 μm band is almost as strong as the 1 μm band. The internal blackish face has lower reflectance, a broader band in the 1 μm region, and a 2 μm band that is much weaker than the 1 μm band. The external face absorbs more infrared light than the other spectra, and in fact has a continuum with a negative slope. Only spectra of chips and whole rock samples have negatively-sloped continua. The 1 μm absorption band is weak and broad. The 2 μm band is barely perceptible in the spectrum of the external face. The powder has a broad 1 μm band and an apparently weak 2 μm band that is superimposed on an increasing continuum with wavelength.

We fit the powder spectrum of this meteorite using a set of startup parameters for eight bands, including a UV absorption edge, four pyroxene bands, and three olivine bands. These were determined from visual inspection of the spectrum, knowledge of the mineralogy of the sample (McSween, Taylor, and Stolper 1979; Ishii, Takeda, and Yanai 1979), and relationships between band parameters and chemical mineralogy of olivine (Sunshine and Pieters 1998) and pyroxenes (e.g., Adams 1974). We were able to fit bands that are consistent with olivine band positions and a pair of low-calcium pyroxene bands with RMS error of 0.012. When we tried to include an olivine and two pyroxenes, the least squares fitting produced a positive band in the 2 μm region, which is not physically realistic.

We next fit 12 bands representing Fo_{75} olivine and three pyroxenes (Fig. 10 and Table 6), as reported in the literature. The resulting fit has a RMS error of 0.009 with olivine and pyroxene bands that are consistent with the chemical mineralogy of the meteorite and established pyroxene trends (Figs. 3a–c), all of which are close to 1 σ of the mean. The band parameters of olivine (Figs. 11a–c) are plotted relative to those derived for terrestrial olivine (Sunshine and Pieters 1998), and are consistent to the point of making the MGM fit realistic with respect to this meteorite's mineral chemistry.

Los Angeles

The reflectance spectrum has the three strong absorption bands characteristic of shergottite meteorites (Fig. 1). It also has similarities to the spectrum of ALH 77005 and appears by eye to contain olivine. We fit the spectrum with two different
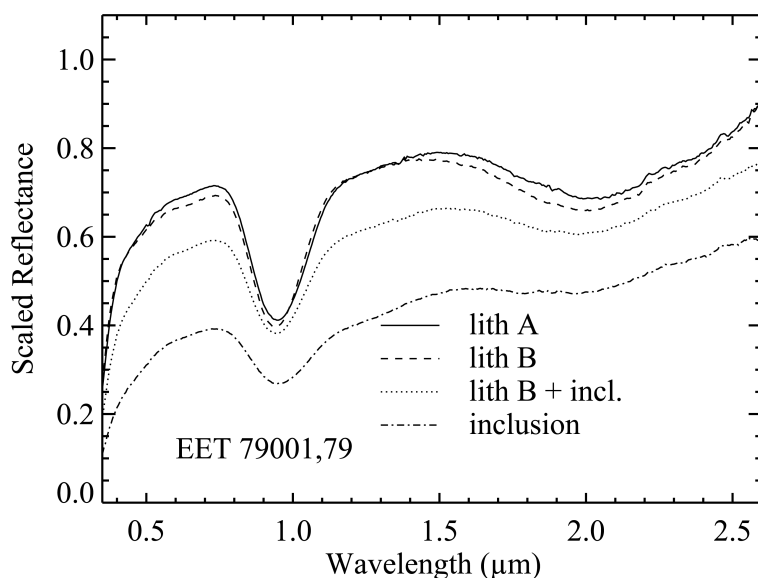
Fig. 6a. Spectra of regions of thin section of EET 79001,79 pictured in the left portion of Fig. 5. From top to bottom, the spectra shown are lithology A, lithology B, lithology B plus inclusion, inclusion alone.
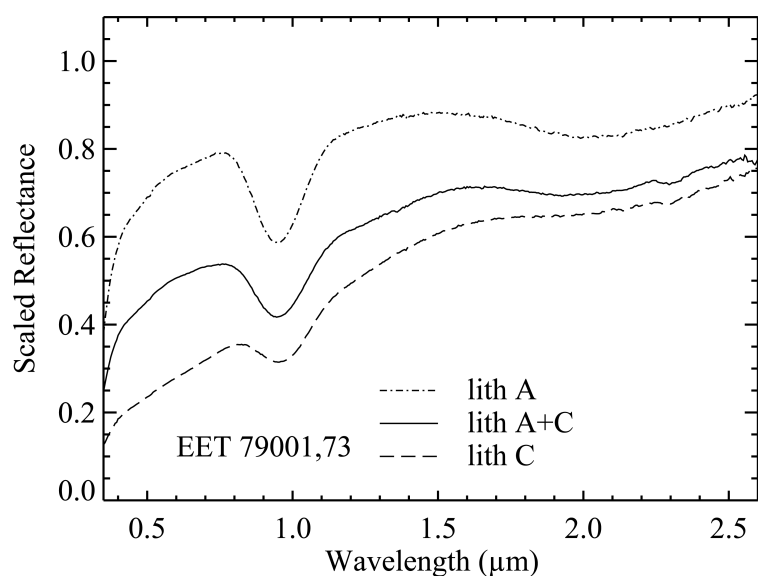

Fig. 6b. Spectra of regions of thin section EET 79001,73 pictured in the right side of Fig. 5. From top to bottom, the spectra are lithology A, lithology A + C, and lithology C alone.

approaches. First, we did a free fit, getting great residuals. However, the relative band strengths were not physically realistic; the fitted 2 μm bands were stronger than the 1 μm bands. Next, we predicted the band positions from the range of pyroxene mineralogy reported in Xirouchakis et al. (2002). The results are not realistic because the relative band depth ratios between the 1 and 2 μm bands are not physically reasonable, according to calibrations of terrestrial pyroxenes. A mathematically satisfactory fit was arrived at by removing two olivine bands required for the fit of ALH 77005, positioning the two 2 μm bands by eye and letting the fit run

to changes in residuals of $<1 \times 10^{-5}$ (Fig. 12). The band parameters are listed in Table 7 with mean residuals of 0.003.

Band centers are plotted in Figs. 3a–c. The center of the longest wavelength band at 2.45 μm falls off the trend in Figs. 3b and 3c. The band centers in Fig. 3a are within 3 σ of the pyroxene trend for the low-calcium pyroxene. In Fig. 3b, the low-Ca pyroxene falls within 1 σ of the trend, but is off the plot (and not plotted) and is >3 σ for the high-calcium pyroxene. This fit is not validated against the mineralogy of this meteorite. This sample requires more detailed investigation of its mineralogy.
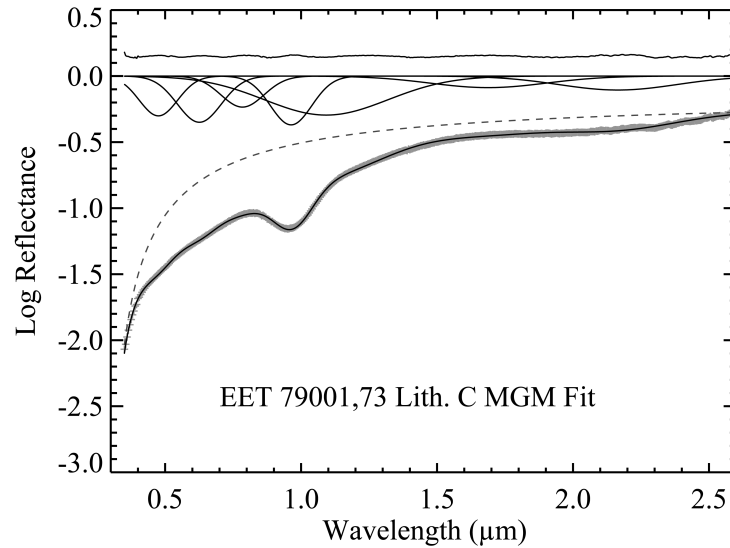
Fig. 7. MGM band fit of thin section of lithology C of EET 79001,73. The spectrum is taken of the dark region of this thin section is shown in Fig. 5 (right). The plots are as described in Fig. 2. Whereas bands can be fit, they are not as strong as in lithology A and B, and the M1 band is very broad.
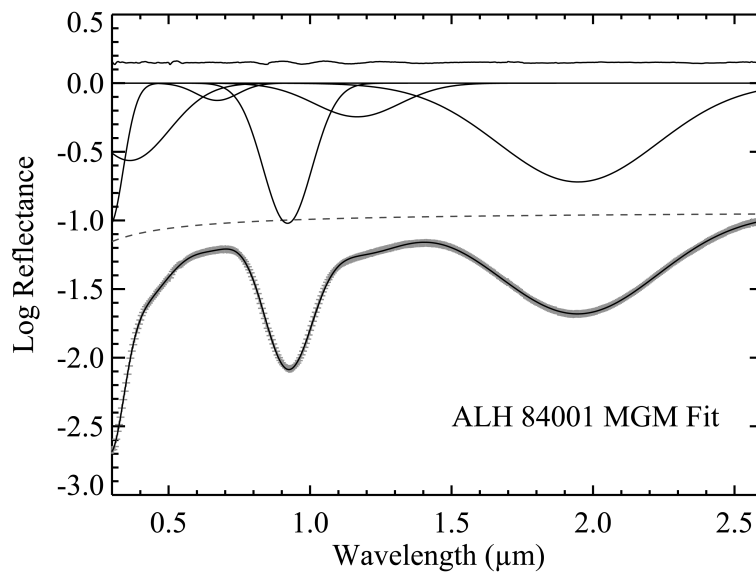

Fig. 8. MGM band fit of powder ALH 84001, a basaltic shergottite mostly consisting of orthopyroxene. Plots are as described in Fig. 2. Only one pyroxene composition can be fit to this spectrum consistent with its mineral composition.

Chassigny

Chassigny has a spectrum dominated by two absorption features: the UV absorption shortward of 0.5 μm and the composite 1 μm olivine band. There is no 2 μm band because this meteorite contains no pyroxene. Two narrow and weak absorptions can be seen in the visible region at 0.455, 0.607 μm (Fig. 1). The strongest band is the UV absorption edge. Six modified Gaussian bands can be fit to this spectrum with mean residuals of 0.008 and changes in the residuals $<1 \times 10^{-7}$ (Fig. 13, Table 8). The positions of these bands are consistent

with band centers of terrestrial olivines (Fig. 11a). The band widths (Fig. 11b) and relative strengths (Fig. 11c) are also consistent with those of terrestrial olivines (Sunshine and Pieters 1998), making the band parameters robust to the composition of the olivine in Chassigny.

Nakhla and Lafayette

The UV edge and the 1 and 2 μm bands are the three dominant absorption bands present in the spectra of both Nakhla and Lafayette (Figs. 14 and 15). The 1 μm band

Table 9. Nakhla powder band parameters.

Band	Mineral	Site	Center (nm)	FWHM	Strength
1	ol/pyx	CT	292.65	144.57	−1.87
2	ol/pyx	CF	431.58	224.16	−0.70
3	ol/pyx	CF	651.86	144.24	−0.23
4	pyx	CF	771.28	146.69	−0.27
5	ol	M1	870.64	144.75	−0.15
6	aug	M2	989.55	174.38	−0.73
7	ol	M2	1067.71	118.06	−0.20
8	aug	M1	1136.90	191.66	−0.16
9	ol	M1	1261.97	383.17	−0.28
10	aug	M2	2309.49	632.21	−0.47

pyx = pyroxene; ol = olivine; aug = augite; FWHM = full width half max. RMS error = 0.00491.

Table 10. Lafayette powder band parameters.

Band	Mineral	Site	Center (nm)	FWHM	Strength
1	pyx	CT	307.26	145.20	−2.09
2	pyx	CF	453.99	211.49	−1.08
3	pyx/ol	CF	634.77	136.49	−0.26
4	pyx	CF	752.04	209.33	−0.37
5	ol	M1	870.60	234.41	−0.15
6	aug	M2	987.03	200.16	−0.84
7	ol	M2	1063.95	128.37	−0.20
8	aug	M1	1138.19	215.73	−0.18
9	ol	M1	1266.88	377.43	−0.38
10	aug	M2	2302.37	684.16	−0.52

pyx = pyroxene; ol = olivine; aug = augite; FWHM = full width half max. RMS error = 0.00896.

complex in both meteorites is at a relatively long wavelength due to the presence of both olivine and a high-calcium pyroxene. The 2 μm band is at long wavelength because the pyroxenes are very iron and calcium rich. A broad plateau in the mid-visible spectrum of Nakhla distinguishes it from the spectrum of Lafayette. The spectra of Nakhla and Lafayette were measured to 3.5 μm. At this long wavelength, there is a complex of telluric OH molecular-vibrational bands that cannot be represented as modified Gaussian bands. The mineral chemistry of both meteorites is such that the 2 μm band overlaps with the 3.5 μm region, compromising the resultant fits. With this in mind, we fit the spectra.

Nakhla

We used a startup file containing the three primary bands of olivine and high-calcium augite to fit the spectrum of Nakhla powder containing olivine and high-Ca augite. Band parameters for the startup file were derived from olivines (Sunshine and Pieters 1998), pyroxenes (Sunshine and Pieters 1993a), and mineral chemistry (Bunch and Reid 1975; Berkeley et al. 1979; Smith, Steele, and Leitch 1983; Mikouchi and Miyamoto 1998). The fit did not pass validation tests because the width of bands at 0.83 and 1.22 μm were 30–40% broader than olivine and pyroxene bands at this wavelength.

Adding two bands in these regions resulted in relative band strengths not consistent with the terrestrial minerals. We carried out two more fits constraining the relative band strengths to those of terrestrial minerals and arrived at the band positions in Fig. 14 and Table 9 for Nakhla. Olivine bands are located at 0.871, 1.068, and 1.262 μm. Their band positions are consistent with those of terrestrial olivines (Fig. 11a). The resulting fit has low residuals (0.005) and a change in residuals <1 × 10^{-5}. The band centers and relative band strengths are consistent with terrestrial olivines (Figs. 11a and 11c); however, the bandwidths are too narrow. The band at 0.77 μm is either a crystal field or charge transfer absorption; the assignment can be debated. The 1.14 μm band

is Fe^{2+} in the M1 site. At 0.989 and 2.309 μm the transitions are due to Fe^{2+} in the M2 site (Figs. 3a, 3b, and 3c).

We were able to fit the spectrum with three bands of olivine and four bands of high-calcium pyroxene. We believe it is necessary to include bands for both the M1 and M2 sites in order to resolve both olivine and pyroxene in the spectrum. Ueda et al. (2002) measured Nakhla and used MGM least squares fitting on three primary absorptions in the 1 and 2 μm region. We show here that it is possible to obtain a good fit, provided that all the crystallographic sites are included in the fitting.

Lafayette

Initial MGM fitting was done with a startup file consisting of the final output from fitting Nakhla. The composition is similar enough to allow the mathematics to account for the spectral differences. Upon validation of the fitted absorptions, the bands between 1.1 and 1.5 μm were wider than terrestrial bands in similar positions in both pyroxene and olivine, and the olivine band depth ratios were not similar to terrestrial olivines. In a second iteration, we constrained the band depths of the olivine bands with little improvement in the fit. A final fit (Fig. 15, Table 10) in which we constrained the position of the olivine bands (Fig. 11a) resulted in a fit with band widths and relative depths that are not consistent with terrestrial olivines (Figs. 11b and 11c) and therefore are not characterized as a robust fit to the mineralogy of the sample. The MGM model does not result in a good fit for this meteorite.

DISCUSSION

In the database of spectral reflectance of meteorites, one would welcome a one-to-one correspondence of meteorite type with reflectance spectrum, permitting a direct association between mineralogy and reflectance. We looked for this among the Shergotty meteorites according to the rationale for meteorite classification of shergottites by Goodrich (2002).
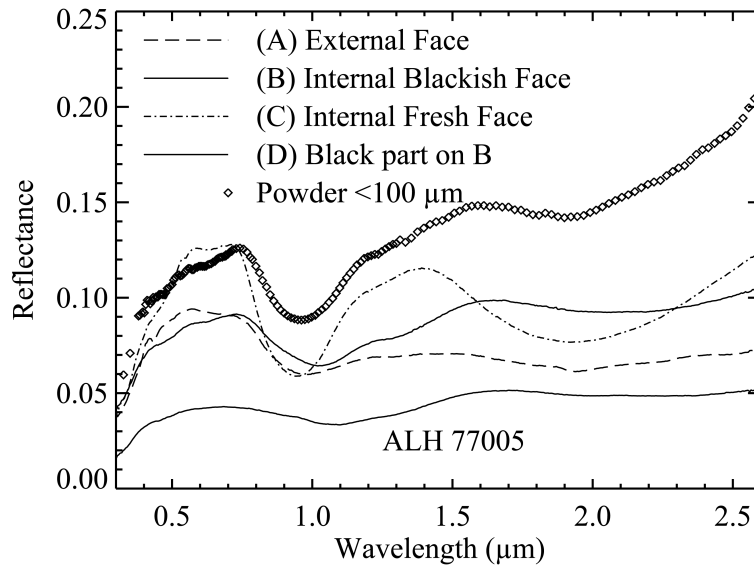
Fig. 9. Spectra of regions of ALH 77005,112, a lherzolitic shergottite containing olivine and three pyroxenes. The sample is a 1 cm piece. From top to bottom looking at 1.2 μm the spectra are of: powder <100 μm, internal fresh face, another internal face of the chip that is blackish, external face of the chip, a sub-sample of the blackish face that is only black in appearance.
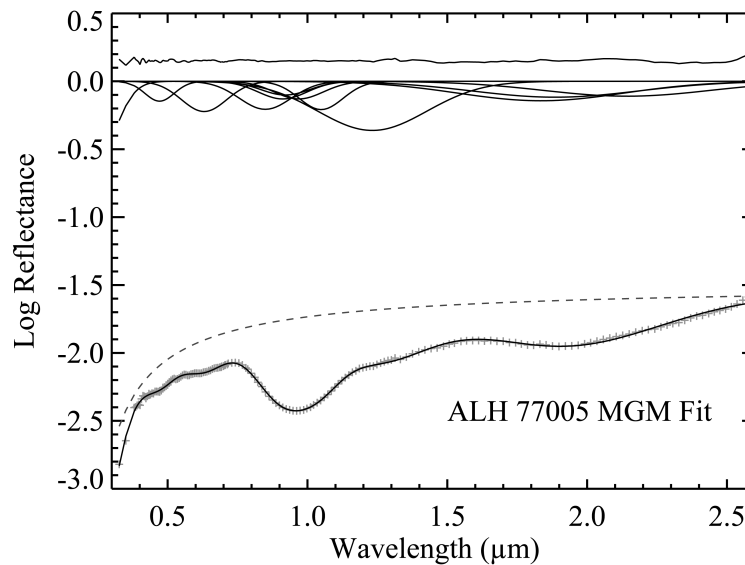

Fig. 10. MGM fit of ALH 77005 powder showing bands attributable to olivine and three pyroxenes. Plots are as described in Fig. 2. The residuals decreased as more bands were added.

There is close similarity in the spectra and band parameters of Shergotty, Zagami, and EET 79001,b, all members of the group of basaltic shergottites (Goodrich 2002). Our spectrum of Los Angeles, which is also a basaltic shergottite, is of a coarsely ground sample and appears significantly different in Fig. 1 than the others of this type. However, the band parameters are all within 3% of the mean for band center, 20% of the mean for band width, and 50% of the mean for band depth. On the other hand, based on mineralogy and petrological factors, one would not place the

spectrum of EET 79001,a (Fig. 6a) in a separate class based on its reflectance spectrum compared to those of other basaltic shergottites (Fig. 1) as Goodrich (2002) proposes. The meteorite (or the sample studied here) does not contain enough olivine to influence the spectrum, though its presence affects its petrological description.

The lherzolitic shergottites, of which ALH 77005 is presented here, do have a distinct spectral reflectance because they contain both olivine and multiple pyroxenes. The nakhlites are distinguished from the lherzolitic
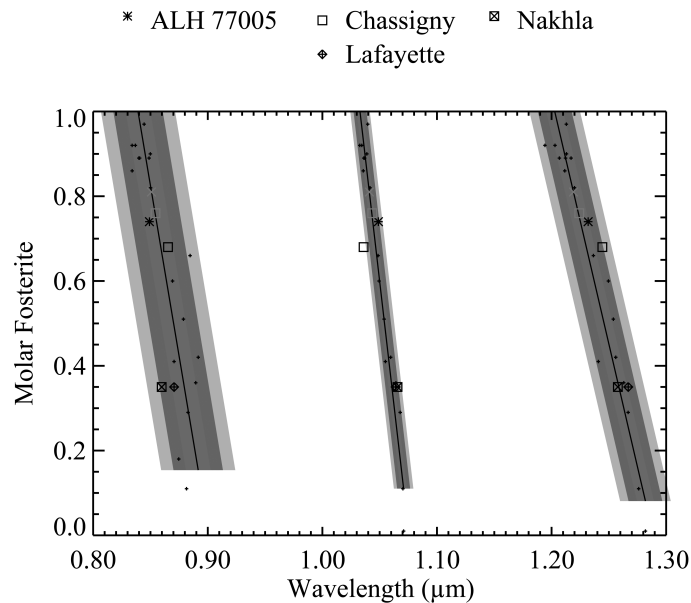
Fig. 11a. Molar % fosterite versus wavelength for powdered terrestrial olivines (after Sunshine and Pieters 1998) shown in small "+"s. Large symbols are the band center positions and composition of olivine absorptions in Martian meteorites containing olivine. Solid lines are the mean of the terrestrial olivines. Shaded areas represent 1 σ, 2 σ, and 3 σ deviations from the mean.
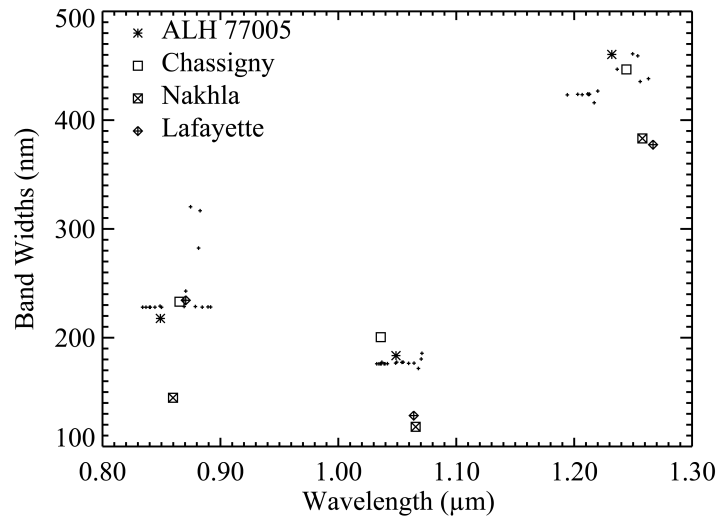

Fig. 11b. Olivine bandwidths versus wavelength of powdered terrestrial olivines, from Sunshine and Pieters (1998) shown in small "+"s. Martian meteorite band widths are in large symbols as noted in the figure legend.

shergottites because the pyroxene in nakhlites is higher in calcium than those of the lherzolitic shergottites (Fig. 1) and influences the spectra by shifting the 2 μm band to much longer wavelength.

Comparison with Previous MGM Fitting of Martian Meteorites

Zagami was measured and fit using MGM analysis by Schade and Wäsch (1999). They report five absorption bands and show that different band parameters can be found from measurements at different locations of the sample. They interpret the differences as representing compositional heterogeneity of the sample. The fit in Table 3 agrees with theirs to within 1–6% for band centers, 1–34% in band width, and 12–68% in band depth. These differences, especially the large one in the case of band strength, illustrate the modeling nature of numerical band fitting and the effect of sample preparation, grinding, and grain size on the band strength in pyroxenes. The band strength, and to some extent the band width, are not intrinsic parameters of the material. However, the constraints on bandwidth need to be considered with respect to crystal field theory and electronic configuration within pyroxene mineral structures. This subject will be taken
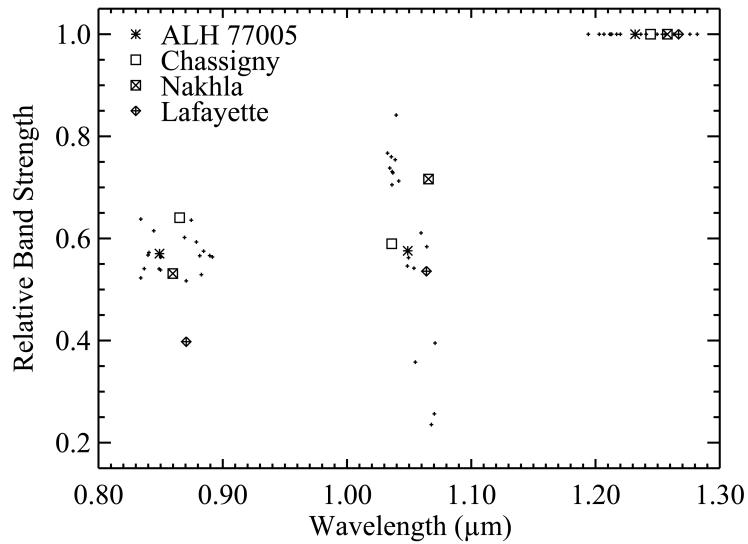
Fig. 11c. Relative band strength versus wavelength of powdered terrestrial olivines (small "+"s) from Sunshine and Pieters (1998) with Martian meteorites in large symbols according to the figure legend. Relative band strength is relative to the long wavelength olivine band.
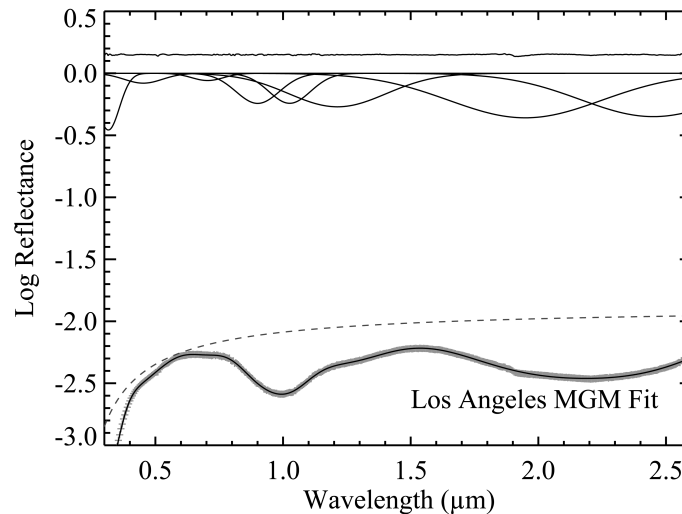

Fig. 12. MGM band fit of course-grained powder of Los Angeles basaltic shergottite composed predominantly of maskelynite and orthopyroxene. The orthopyroxene ($En_{50-6}Fs_{81-33}Wo_{12-41}$ [Xirouchakis et al. 2002]) signatures are found in the spectrum. Plots are as described in Fig. 2.

up in subsequent research. The band centers are presently the best compositionally diagnostic spectral feature for identifying sources of Martian meteorites on Mars.

In previous analyses of Nakhla (Schade and Wäsch 1999; Ueda et al. 2002), the MGM analysis did not include an absorption band for each crystallographic site that produces absorption bands. As a result, completely different band parameters are arrived at in the analysis presented here. The lack of similar fitting methodologies prevents a comparison between our fit and previously published band parameters. The fitting approach used here is based on knowledge of the sample and is not a blind fit. It is a closer representation of the components found in the Nakhla meteorite and can be used to

test spectra of regions of Mars for signatures that are representative of Nakhlites.

The previous analysis of EET 79001 (Sunshine et al. 1993) was built upon in this work by showing the variation in spectrum and band parameters as a function of petrology that can be targeted when measuring regions of a thin section. The largest differences between the spectrum of a powder and a thin section of comparable mineralogy is in the strength of the absorption band (Table 4), where the band strengths can be 25% to >100% stronger in a powder than a thin section of the same material. This can be explained in terms of the larger number of grains with which photons interact in a powdered sample versus the many fewer when passing through a thin
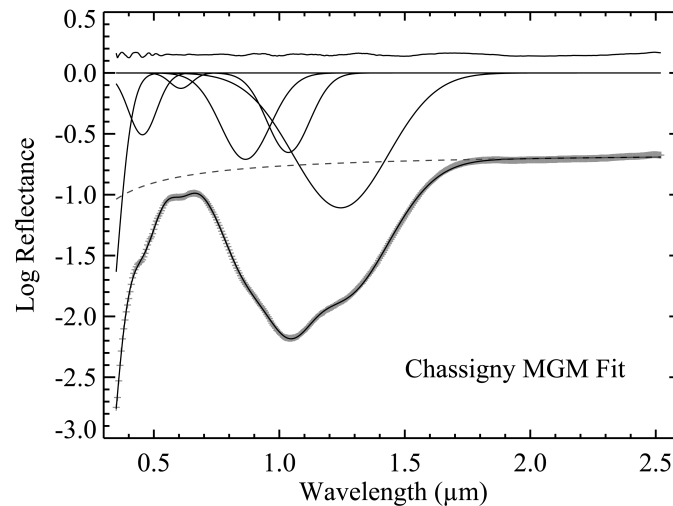
Fig. 13. MGM band fit of Chassigny powder consisting of monomineralic olivine. Plots are as described in Fig. 2.
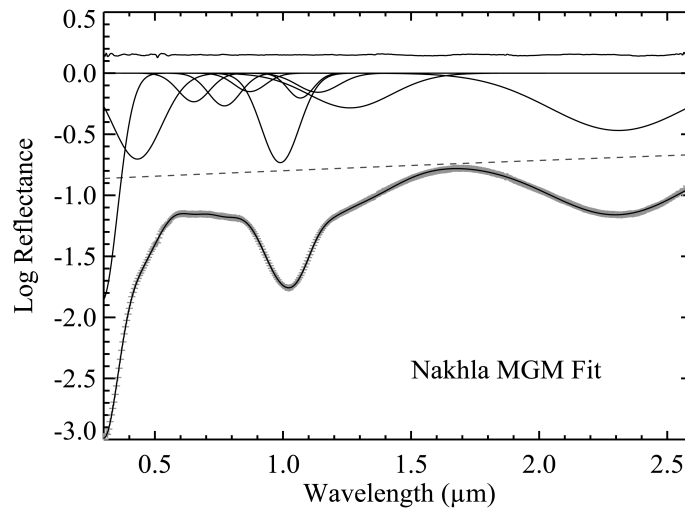

Fig. 14. MGM band fit of Nakhla powder consisting of olivine and Ca-rich augite. Plots are as described in Fig. 2.

section of a finite and small thickness (standard thickness is 0.03 mm). The results shown here demonstrate that thin sections can be used to derive the scattering properties of minerals and meteorite samples when measured at different angles of incidence and emission. From the range of spectra measured at different geometry, scattering parameters can be derived and, the reflectance of a regolith can be predicted.

The Matter of the Continuum

It is important to emphasize that physically validated band parameters were derived only when the continuum was not tangent to the spectrum. In simple and empirical band analysis approaches, the continuum is always tangent to the spectrum. A physical theory for modeling the continuum is needed to move this modeling process forward. That the continuum is not tangential to the spectrum calls into question

other band analysis approaches that define the continuum as tangent to the spectrum (e.g., Cloutis et al. 1986; McFadden et al. 2001). This point has been noted previously and demonstrated with mixtures of mafic silicates and opaque phases that are spectrally neutral (Moroz and Arnold 1999).

Applications for These Band Parameters

Hamilton et al. (1997) studied thermal emission spectra of four Martian meteorites, noting the similarities and differences in their restrahlen bands. Bishop and Hamilton (2001) have combined analysis of reflectance and emittance spectra of Martian meteorites to provide more direct information about Martian surface composition. Combining a wider range of spectral data holds promise for finding combinations of features that are diagnostic of these meteorite types and can be used to locate the source regions
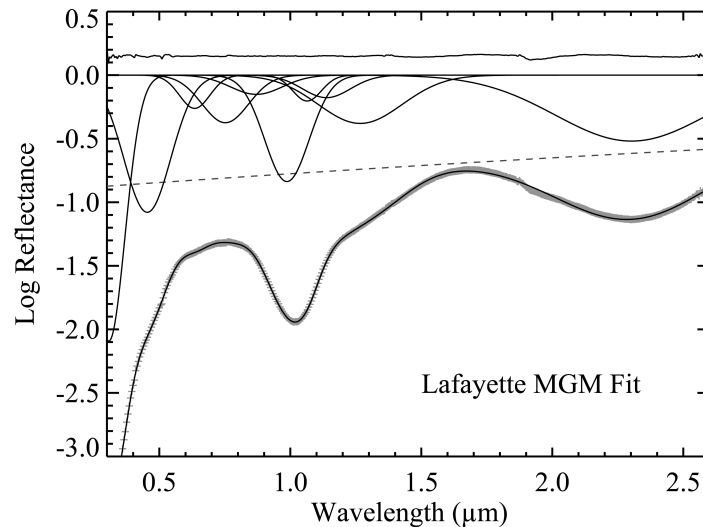
Fig. 15. MGM band fit of Lafayette powder consisting of olivine and Ca-rich augite. Plots are as described in Fig. 2.

of the Martian meteorites. It seems that finding emission bands associated with Si-O bond length (and therefore mineral chemistry) and tying those to the visible and near-IR absorption features, which also are controlled by bond length, would allow sufficient constraints to generate a robust mineral interpretation of Martian crustal composition. Emissions band attributed to plagioclase feldspars are identified with TES spectra and add an additional mineral that can be used to constrain composition. None of the absorption bands in the 0.3–2.6 μm region are attributable to plagioclase.

The derived band parameters can be used to fit spectra of Mars to test for the presence of the minerals and chemistry of those found among the SNC group of meteorites. One caveat is that the band depths particularly vary with grain size and the number of grains encountered by a photon (powder, chip, or thin section), and thus the band parameters are not those of the single particle scattering component of the assemblage. Another set of laboratory experiments through a range of viewing geometry and grain sizes is needed to determine the single particle scattering albedo of a sample's spectrum as well as multiple scattering parameters. Knowledge of the band parameters found among the range of known Martian meteorites is useful for constraining the composition of relatively unweathered portions of the surface of Mars, that are pulverized as opposed to bedrock, where 1 and 2 μm bands can be resolved.

In 2004–05, data returned from the OMEGA instrument on board Mars Express provides spectra between 0.35 and 5.2 μm at spatial resolutions ranging from 300 m to 5 km (e.g., Puget et al. 1995, Bibring et al. 2004). Another instrument with adequate spectral and spatial resolution for surface mineralogy on Mars is the CRISM, under development for NASA's Mars Reconnaissance Orbiter (MRO), scheduled for launch in 2005 (e.g., Murchie et al. 2002).

Possible craters from which these meteorites have been ejected have been cited (Barlow 1997; Mouginis-Mark et al. 1992) based on the meteorites' ejection ages, which were derived from isotopic analysis. The two craters located by Barlow (1997) should be targets for Mars missions in the future. They are at 11.7°S, 243.3°W east of Hesperia Planitia and 14.0°S, 343.5°W south of the Schiaparelli impact basin. Other plausible source regions are young flows in the Elysium area, in Syrtis Major, or in dark areas of basaltic composition (Mustard et al. 1997). Rayed craters are also considered relatively dust free and may be a place to look. With identification of the source of any of the Martian meteorites, an absolute age scale will be connected with Martian chronology, thus providing a vital dimension in the study of the history of Mars and evolution of our solar system.

CONCLUSIONS

The mineralogy and petrology of Martian meteorites produce reflectance spectra that are distinguishable from each other and are unique compared to spectra of other meteorite types. The strong absorption bands due to crystalline mafic silicates are ready indicators of the dominant mineralogy of these meteorites.

Modified Gaussian absorption bands can be fit to the spectrum with mean residuals (<0.009), provided an absorption band is included for each crystallographic site at which cations absorb photons, and are present in detectable abundance.

Physically validated absorption band parameters can be found when the continuum is not tangential to the spectrum and has a positive slope, not a negative slope. The poor fits of Lafayette and Los Angeles exist when the continuum is difficult to characterize.

It was demonstrated that thin sections placed on top of

halon can be used to measure reflectance spectra and extract band parameters that correlate with the mineralogy of the region of the thin section, which was measured to better than 10% for band center and width. The depth of absorption bands is highly dependent on multiple scattering and varies between thin section, powders, chips, and slabs. The advantage of measuring spectra of thin sections is that the sample can be controlled and studied with optical microscopy. Whereas the band parameters derived here are not unique to the spectrum, they are consistent with the mineralogy of the meteorites and the band parameter systematics derived from samples with geochemical analysis. These band parameters can be used to constrain interpretations of spectra from Mars with similar spectral resolution and high spatial resolution.

Editorial Handling—Dr. Carlé Pieters

REFERENCES

Adams J. B. 1974. Visible and near-infrared diffuse reflectance spectra of pyroxenes as applied to remote sensing of solid objects in the solar system. *Journal of Geophysical Research* 79:4829–4836.

Adams J. B. 1975. Interpretation of visible and near-infrared diffuse reflectance spectra of pyroxenes and other rock forming minerals. In *Infrared and raman spectroscopy of lunar and terrestrial materials*, edited by Karr C. San Diego, California: Academic Press. pp. 91–116.

Barlow N. G. 1997. Identification of possible source craters for the Martian meteorites ALH 84001. Proceedings, SPIE Annual Meeting 1997. pp. 26–35.

Berkely J. L., Keil K., Prinz M., and Gomes C. B. 1979. The Governador Valadares nakhlite and its relationship to other nakhlites (abstract). 10th Lunar and Planetary Science Conference. p. 103.

Bibring, J. P. The Omega Team 2004. The Omega/Mars Express First Results 2004 LPI35.2173B.

Bishop J. L. and Hamilton V. E. 2001. Spectroscopic detection of minerals in Martian meteorites using reflectance and emittance spectroscopy and applications to surface mineralogy on Mars (abstract #P52B-0580). 2001 AGU Fall Meeting. *Eos Transactions* 82(47).

Bishop J. L., Mustard J. F., Pieters C. M., and Hiroi T. 1998a. Recognition of minor constituents in reflectance spectra of Allan Hills 84001 chips and the importance for remote sensing on Mars. *Meteoritics & Planetary Science* 33:693–698.

Bishop J. L., Pieters C. M., Hiroi T., and Mustard J. F. 1998b. Spectroscopic analysis of Martian meteorite Allan Hills 84001 powder and applications for spectral identification of minerals and other soil components on Mars. *Meteoritics & Planetary Science* 33:699–707.

Bogard D. D. and Johnson P. 1983. Martian gases in an Antarctic meteorite? *Science* 221:651–654.

Bogard D. D., Nyquist L. E., and Johnson P. 1984. Noble gas contents of shergottites and implications for the Martian origin of SNC meteorites. *Geochimica et Cosmochimica Acta* 48:1723–1739.

Bunch T. E. and Reid A. M. 1975. The nakhlites. I—Petrography and mineral chemistry. *Meteoritics* 10:305–315.

Burns R. G. 1993. *Mineralogical applications of crystal field theory*, 2nd edition. New York: Cambridge University Press. 551 p.

Clayton R. N. 1993. Oxygen isotope analysis. In Antarctic Meteorite Newsletter 16(3), edited by Score R. and Huston L. M. Houston, Texas: Johnson Space Center. pp. 4.

Cloutis E. A., Gaffey M. J., Jackowski T. L., and Reed K. L. 1986. Calibrations of phase abundance, composition, and particle size distribution for olivine-orthopyroxene mixtures from reflectance spectra. *Journal of Geophysical Research* 91:11,641–11,653.

Cloutis E. A. and Gaffey M. J. 1991. Pyroxene spectroscopy revisited: Spectral-compositional correlations and relationship to geothermometry. *Journal of Geophysical Research* 96:22,809–22,826.

Cloutis E. A. 2002. Pyroxene reflectance spectra: Minor absorption bands and effects of elemental substitutions. *Journal of Geophysical Research* 107:doi 10.1029/2001JE001590.

Cloutis E. A., Sunshine J. M., Morris R. V. 2004. Spectral reflectance-compositional properties of spinels and chromites: Implications for planetary remote sensing and geothermometry. *Meteoritics & Planetary Science* 39:545–565.

Floran R. J., Prinz M., Hlava P. F., Keil K., Nehru C. E., and Hinthorne J. R. 1978. The Chassigny meteorite: A cumulate dunite with hydrous amphibole-bearing melt inclusions. *Geochimica et Cosmochimica Acta* 42:1213–1229.

Gaffey M. J. 1976. Spectral reflectance characteristics of the meteorite classes. *Journal of Geophysical Research* 81:905–920.

Goodrich C. A. 2002. Olivine-phyric Martian basalts: A new type of shergottite. *Meteoritics & Planetary Science* 37:B31–B34.

Hale V. P. S., McSween H. Y., and McKay G. A. 1999. Reevaluation of intercumulus liquid composition and oxidation state for the Shergotty meteorite. *Geochimica et Cosmochimica Acta* 63:1459–1470.

Hamilton V. E., Christensen P. R., and McSween H. Y. 1997. Determination of Martian lithologies and mineralogies using vibrational spectroscopy. *Journal of Geophysical Research* 102:25,592–25,603.

Harvey R. P. and McSween H. Y. 1992. Petrogenesis of the nakhlite meteorites—Evidence from cumulate mineral zoning. *Geochimica et Cosmochimica Acta* 56:1655–1663.

Hazen R. M., Bell P. M., and Mao H. K. 1978. Effects of compositional variation on absorption spectra of lunar pyroxenes. Proceedings, 9th Lunar and Planetary Science Conference. pp. 2919–2934.

Ishii T., Takeda H., and Yanai K. 1979. Pyroxene geothermometry applied to a three-pyroxene achondrite from Allan Hills, Antarctica and ordinary chondrites. *Mineralogical Journal* 9:460–481.

King T. V. V. and Ridley W. I. 1987. Relation of the spectroscopic reflectance of olivine to mineral chemistry and some remote sensing implications. *Journal of Geophysical Research* 92:11,457–11,469.

Laul J. C. 1986. The Shergotty Consortium and SNC meteorites: An overview. *Geochimica et Cosmochimica Acta* 50:875–887.

Lodders K. 1998. A survey of SNC meteorite whole-rock compositions. *Meteoritics & Planetary Science* 33:A183–190.

McFadden L. A., Wellnitz D. D., Schnaubelt M., Gaffey M. J., Bell III J. F., Izenberg N., Murchie S., and Chapman C. R. 2001. Mineralogical interpretation of reflectance spectra of Eros from

NEAR near-infrared spectrometer low phase flyby. *Meteoritics & Planetary Science* 36:1711–1726.

McKay D. S., Gibson E. K., Thomas-Keprta K. L., Vali H., Romanek C. S., Clemett S. J., Chiller X. D. F., Maechling C. R., and Zare R. N. 1996. Search for past life on Mars: Possible relic biogenic activity in Martian meteorite ALH 84001. *Science* 273:924–930.

McSween H. Y., Taylor L. A., and Stolper E. 1979. Allan Hills 77005—A new meteorite type found in Antarctica. *Science* 204:1201–1203.

McSween H. Y. and Jarosewich E. 1983. Petrogenesis of the Elephant Moraine A79001 meteorite: Multiple magma pulses on the shergottite parent body. *Geochimica et Cosmochimica Acta* 47:1501–1513.

McSween H. Y. 1985. SNC meteorites—Clues to Martian petrologic evolution? *Reviews of Geophysics* 23:391–416.

McSween H. Y. 2002. The rocks of Mars, from far and near. *Meteoritics & Planetary Science* 37:7–25.

Mikouchi T. and Miyamoto M. 1998. Pyroxene and olivine microstructures in nakhlite Martian meteorites: Implications for their thermal history (abstract #1574). 29th Lunar and Planetary Science Conference. CD-ROM.

Mittlefehldt D. W. 1994. ALH 84001, a cumulate orthopyroxene member of the Martian meteorite clan. *Meteoritics* 29:214–221.

Moroz L. and Arnold G. 1999. Influence of neutral components on relative band contrasts in reflectance spectra of intimate mixtures: Implications for remote sensing 1. Nonlinear mixing modeling. *Journal of Geophysical Research* 104:14,109–14,121.

Mouginis-Mark P. J., McCoy T. J., Taylor G. J., and Keil K. 1992. Martian parent craters for the SNC meteorites. *Journal of Geophysical Research* 97:10,213–10,225.

Murchie S. et al. 2002. CRISM: Compact Reconnaissance Imaging Spectrometer for Mars on the Mars Reconnaissance Orbiter (abstract #1697). 33rd Lunar and Planetary Science Conference. CD-ROM.

Mustard J. F. and Sunshine J. M. 1995. Seeing through the dust—Martian crustal heterogeneity and links to the SNC meteorites. *Science* 267:1623–1626.

Mustard J. F., Murchie S., Erard S., and Sunshine J. 1997. In situ compositions of Martian volcanics: Implications for the mantle. *Journal of Geophysical Research* 102:25,605–25,616.

Pieters C. M. 1983. Strength of mineral absorption features in the transmitted component of near-infrared reflected light—First results from RELAB. *Journal of Geophysical Research* 88:9534–9544.

Pieters C. M. 1996. Plagioclase and maskelynite diagnostic features (abstract). 27th Lunar and Planetary Science Conference. pp. 1031–1032.

Puget P., Beney J. L., Bibring J. P., Langevin Y., Semery A., and Soufflot A. 1995. OMEGA IR spectral imager for Mars 96 mission SPIE 2583:323:330.

Rossman G. R. 1980. Pyroxene spectroscopy. In *Pyroxenes*, edited by Prewitt C. T. Reviews in mineralogy, vol. 7. Washington D. C.: Mineralogical Society of America. pp. 91–116.

Rubin A. E., Warren P. H., Greenwood J. P., Verish R. S., Leshin L. A., and Hervig R. L. 2000. Petrology of Los Angeles: A new basaltic shergottite find (abstract #1963). 31st Lunar and Planetary Science Conference. CD-ROM.

Schade U. and Wäsch R. 1999. Near-infrared reflectance spectra from bulk samples of the two SNC meteorites Zagami and Nakhla. *Meteoritics & Planetary Science* 34:417–424.

Singer R. B. 1981. Near-infrared spectral reflectance of mineral mixtures: Systematic combinations of pyroxenes, olivine, and iron oxides. *Journal of Geophysical Research* 86:7967–7982.

Smith J. V., Steele I. M., and Leitch C. A. 1983. Mineral chemistry of the shergottites, nakhlites, Chassigny, Brachina, pallasites and ureilites. Proceedings, 14th Lunar and Planetary Science Conference. *Journal of Geophysical Research* 88:B229–B236.

Stöffler D., Ostertag R., Jammes C., Pfannschmidt G., Sen Gupta P. R., Simon S. B., Papike J. J., and Beauchamp R. H. 1986. Shock metamorphism and petrography of the Shergotty achondrite. *Geochimica et Cosmochimica Acta* 50:889–903.

Stolper E. M. and McSween H. Y. 1979. Petrology and origin of the shergottite meteorites. *Geochimica et Cosmochimica Acta* 43:589–602.

Sunshine J. M. and Pieters C. M. 1990. Extraction of compositional information for olivine reflectance spectra: A new capability for lunar exploration (abstract). 21st Lunar and Planetary Science Conference. pp. 1263–1264.

Sunshine J. M., Pieters C. M., and Pratt S. F. 1990. Deconvolution of mineral absorption bands: An improved approach. *Journal of Geophysical Research* 95:6955–6966.

Sunshine J. M. and Pieters C. M. 1993a. Estimating modal abundances from the spectra of natural and laboratory pyroxene mixtures using the modified Gaussian model. *Journal of Geophysical Research* 98:9075–9087.

Sunshine J. M. and Pieters C. M. 1993b. Determining the composition olivine on asteroidal surfaces (abstract). 24th Lunar and Planetary Science Conference. pp. 1379–1380.

Sunshine J. M., McFadden L. A., and Pieters C. M. 1993. Reflectance spectra of the Elephant Moraine A79001 meteorite: Implications for remote sensing of planetary bodies. *Icarus* 105:79–91.

Sunshine J. M. and Pieters C. M. 1998. Determining the composition of olivine from reflectance spectroscopy. *Journal of Geophysical Science* 103:13,675–13,688.

Treiman A. H. and Sutton S. R. 1992. Petrogenesis of the Zagami meteorite: Inferences from synchrotron X-ray fluorescence (SXRF) microprobe and electron microprobe analyses of pyroxenes. *Geochimica et Cosmochimica Acta* 56:4059–4074.

Treiman A. H., Gleason J. D., and Bogard D. D. 2000. The SNC meteorites are from Mars. *Planetary and Space Science* 48:1213–1230.

Ueda Y., Mikouchi T., Miyamoto M., and Hiroi T. 2002. First analysis of the reflectance spectrum of Yamato-000593: The spectroscopic similarity between Yamato-000593 and Nakhla. *Proceedings of the NIPR Symposium on Antarctic Meteorites* 15. pp. 171–173.

Weidner V. R. and Hsia J. J. 1981. Reflection properties of pressed polytetrafluoroethylene powder. *Journal of the Optical Society of America* 71:856–861.

Xirouchakis D., Draper D. S., Schwandt C. S., and Lanzirotti A. 2002. Crystallization conditions of Los Angeles, a basaltic Martian meteorite. *Geochimica et Cosmochimica Acta* 66:1867–1880.